Phys Chem Minerals (1992) 19:307–321

PHYSICS AND CHEMISTRY OF MINERALS

Dynamics of the α-β Phase Transitions in Quartz and Cristobalite as Observed by In-Situ High Temperature ^{29}Si and ^{17}O NMR

Dane R. Spearing, Ian Farnan, and Jonathan F. Stebbins

Department of Geological and Environmental Sciences, Stanford University, Stanford, CA 94305, USA

Received November 25, 1991 / Revised, accepted June 8, 1992

Abstract. Relaxation times (T_1) and lineshapes were examined as a function of temperature through the α-β transition for ^{29}Si in a single crystal of amethyst, and for ^{29}Si and ^{17}O in cristobalite powders. For single crystal quartz, the three ^{29}Si peaks observed at room temperature, representing each of the three differently oriented SiO_4 tetrahedra in the unit cell, coalesce with increasing temperature such that at the α-β transition only one peak is observed. ^{29}Si T_1's decrease with increasing temperature up to the transition, above which they remain constant. Although these results are not uniquely interpretable, hopping between the Dauphiné twin related configurations, α_1 and α_2, may be the fluctuations responsible for both effects. This exchange becomes observable up to 150° C below the transition, and persists above the transition, resulting in β-quartz being a time and space average of α_1 and α_2. ^{29}Si T_1's for isotopically enriched powdered cristobalite show much the same behavior as observed for quartz. In addition, ^{17}O T_1's decrease slowly up to the α-β transition at which point there is an abrupt 1.5 order of magnitude drop. Fitting of static powder ^{17}O spectra for cristobalite gives an asymmetry parameter (η) of 0.125 at room T, which decreases to <0.040 at the transition temperature. The electric field gradient (EFG) and chemical shift anisotropy (CSA), however, remain the same, suggesting that the decrease in η is caused by a dynamical rotation of the tetrahedra below the transition. Thus, the mechanisms of the α-β phase transitions in quartz and cristobalite are similar: there appears to be some fluctuation of the tetrahedra between twin-related orientations below the transition temperature, and the β-phase is characterized by a dynamical average of the twin domains on a unit cell scale.

Introduction

Quartz and cristobalite, two polymorphs of SiO_2, undergo what were once considered classic second-order displacive phase transitions at 573° C and about 270° C, respectively. Since it was first observed by La Chatelier (1889), the α-β phase transition in quartz has been intensively studied using a wide variety of techniques. There has been a renewed interest in the phase transition, and in particular its mechanism and dynamics, since the discovery of the incommensurate phase (INC) in quartz by Bachheimer (1980). It is now known that the "classic" second-order α-β phase transition in quartz is actually two transitions: the first-order α-INC transition, and the second order INC-β transition, separated by about 1.8° C (Hatta et al. 1985). Despite the increased research and interest in the quartz transition, there still remains some controversy over the nature of the β-quartz structure and pre-transitional structural dynamics in α-quartz. TEM studies on the α-β quartz transition (van Tendeloo et al. 1976; Heaney and Veblen 1991) suggest that β-quartz has a dynamic structure, while a recent hyper-Raman scattering experiment (Tezuka et al. 1991) indicates that the α-β phase transition is well described by a simple displacive-type mechanism and that the β-quartz structure is static. While no incommensurate phase has yet been detected in cristobalite, recent symmetry calculations based on Landau theory (Hatch and Ghose 1991) and optical transform and Monte Carlo studies (Welberry et al. 1989) suggest that β-cristobalite is a dynamically averaged structure as well. The purpose of this study was to examine both the α-β quartz and α-β cristobalite phase transitions using nuclear magnetic resonance (NMR) to resolve some of the questions about their dynamical nature and the structural state (dynamic or static) of the high temperature phases. ^{29}Si relaxation time (T_1) measurements and line shape studies were used to examine the quartz transition, while ^{29}Si MAS and ^{17}O static T_1 and line shape studies were used to examine the cristobalite transition.

Quartz

The α-β phase transition in quartz is characterized by the loss of a two-fold symmetry axis parallel to **c** with

decreasing temperature resulting in a symmetry change from the β-quartz space groups $P6_222$ or $P6_422$ to the α-quartz space groups $P3_221$ or $P3_121$ (right and left handed, respectively). The transition temperature for pure quartz is 573.3° C with a minor dependence ($\pm$ 1.5° C) on composition and growth temperature (Tuttle 1949). In a static model, this loss of symmetry is attributed to a rotation around the two-fold symmetry axis of the rigid SiO_4 tetrahedra perpendicular to the **c**-axis. However, evidence that this transition is characterized by large amplitude vibrations of the oxygen tetrahedra was first presented by Raman and Nedungadi (1940) when they observed a broadening of the 220 cm^{-1} line with increasing temperature in their scattered light (Raman) experiments.

Extensive single crystal and powder x-ray diffraction (XRD) (Young 1962; Young and Post 1962; Kihara 1990) has shown that there is a marked increase of the oxygen thermal ellipsoid, which also rotates to an orientation perpendicular to the Si-O-Si plane with increasing temperature. These increases in the thermal ellipsoid are related to a vibration of the oxygen atoms perpendicular to the Si-O-Si plane that reaches its maximum amplitude just above the α-β transition. Since the direction of the oxygen vibration is along the line joining the Dauphiné twin related positions, one would expect the mobility and abundance of twin related domains to increase with increasing temperature. Electron microscopy and electron diffraction observations (van Tendeloo et al. 1976; van Goethem et al. 1977; Heaney and Veblen 1991) have confirmed this, and show that these twin-related domains disappear altogether above the INC-β transition temperature. Inelastic neutron scattering experiments on β-quartz (Axe and Shirane 1970; Boysen et al. 1980) have shown there to be a softening of the 207 cm^{-1} mode with increasing temperature, and this has been correlated with an oscillatory rotation of the SiO_4 tetrahedra. From single crystal neutron diffraction, Wright and Lehmann (1981) concluded that the high-symmetry displacive limit of the ideal β-quartz is not achieved as a stable structure, but rather exists as a dynamic average of the classical Dauphiné twin domains of α-quartz. They further concluded that the motion of the SiO_4 tetrahedra that gives rise to this dynamically averaged β-quartz structure is such that the SiO_4 tetrahedra are not distorted (provided that the motions are correlated), and that this motion is on a much longer time scale than typical thermal vibrations, corresponding to a very low frequency lattice mode. Most importantly, the structure as derived from neutron diffraction suggests that the transition is an order-disorder type, where the dominant local site symmetry in the high temperature phase is that of the low temperature α-quartz. Molecular dynamics simulations of the phase transition are also in agreement with this conclusion (Tsuneyuki et al. 1990). The ideal β-quartz phase is thus a transitory phenomenon occurring only when the α-structure flips between the Dauphiné twin related configurations. Hence, the β-phase can be thought of as a time-averaged structure of the two Dauphiné twin domains of α-quartz, or as α-quartz possessing a very large number of Dauphiné twin domains with infinitesimal thickness (Liebau and Böhm 1982; Ghiorso et al. 1979). On the other hand, in a recent study of the quartz transition using hyper-Raman scattering, Tezuka et al. (1991) concluded that a structural fluctuation between the Dauphiné twin related configurations, α_1 and α_2, in β-quartz does not exist above 590° C, although it may occur in the vicinity of the phase transition.

Cristobalite

Cristobalite is the stable polymorph of SiO_2 from 1470° C up to its melting point at 1728° C, but can exist metastably down to around 220 to 270° C where it undergoes the β to α (cubic to tetragonal) displacive phase transition. XRD refinements of the structure (Wyckoff 1925; Dollase 1965; Peacor 1973) show the β-phase to have the cubic space group $Fd\bar{3}m$, whereas the low temperature α-phase is in the tetragonal space group $P4_12_12$, or its enantiomorph $P4_32_12$. The symmetry change from $Fd\bar{3}m$ to $P4_12_11$ (or $P4_32_11$) involves a loss of the three-fold axes, inversion center, and translation vectors $1/2<110>$. The transition temperature in cristobalite is highly variable and shows considerable hysteresis upon cooling. Transition temperatures can range from 130° C to 270° C, although the typical range is between 220° C and 270° C (Hill and Roy 1958). Composition (Perrotta et al. 1989), and synthesis temperature (Hill and Roy 1958) both have an effect on the transition temperature.

Initial x-ray powder refinement of β-cristobalite (Wyckoff 1925) placed it in the cubic space group $Fd\bar{3}m$, with a 180° Si-O-Si bond angle and Si-O bond distance of 1.54 Å (the so called "C9" structure). Nieuwenkamp (1937) showed that the best fit of the x-ray data was obtained by placing the oxygen atom on a circle of radius 0.3 to 0.55 Å, with a six- or twelve-fold disorder and the plane of the circle bisecting the Si-Si axis. Later x-ray refinements placed the oxygen atom in the 96(h) site of the $Fd\bar{3}m$ space group with a 1/6 occupancy (Peacor 1973; Wright and Leadbetter 1975). This refinement was also in better agreement with the Si-O-Si bond angles and Si-O bond distances for other forms of silica. Peacor (1973) concluded that the oxygens are probably dynamically disordered among the 6 possible 96(h) sites in β-cristobalite; however, based on x-ray diffraction alone, he could not distinguish between static or dyamic disorder. Cristobalite, like quartz, twins readily upon cooling from the high temperature phase. A TEM electron diffraction study shows that a complex array of twins on both the fine (200–300 Å) and coarse (several μm) scales exists in α-cristobalite, and that these twins disappear upon heating to the high temperature phase (Withers et al. 1989). Wright and Leadbetter (1975) suggested the disorder in β-cristobalite to be a twinning of ordered domains on a scale comparable to unit cell dimensions. However, a recent Monte Carlo study of the disorder in β-cristobalite (Welberry et al. 1989) concluded that the oxygen atoms are uniformly distributed around an annulus that encircles the 16(c) sites of the $Fd\bar{3}m$ structure, and that if the oxygen atoms do prefer-

entially occupy the six 96(h) sites, this tendency is not very pronounced. Although no definitive conclusion has yet been reached about whether the observed β-cristobalite structure is a static or dynamically averaged structure, symmetry analysis of the phase transition based on Landau theory (Hatch and Ghose 1991) strongly suggests that the α-β cristobalite transition is a fluctuation-induced first-order phase transition and the β-cristobalite structure is a dynamic average of α-cristobalite type domains. That study further concluded that β-cristobalite can be described by a model with twelve local potential energy minima and microscopic domains resonating among the twelve distinct domain configurations. In this model, the ideal C9 structure is never attained at any temperature. The nature of the fluctuations in both the quartz and cristobalite phase transitions, and the dynamical character of both high temperature polymorphs, is the subject of our investigation.

NMR and Phase Transitions

Nuclear magnetic resonance (NMR) is an ideal technique to examine the dynamics of a structure, since it is sensitive to local site geometries around a given nucleus rather than to the structure of the bulk sample. NMR has been used extensively to study the dynamics of phase transitions in crystalline solids (Borsa and Rigamonti 1990; Rigamonti 1984; Blinc 1981). However, it has not yet been widely applied to the study of phase transitions in silicates.

There are essentially two methods of investigation using NMR to examine a solid material: line shape and relaxation time studies. Line shape studies involve examining the shape and position of the resonance peak(s) and can give information about the symmetry and coordination of the environment surrounding the nuclei. For phase transitions, such information is useful in examining structural changes from one phase to another. Such techniques have been used, for example, to examine the α-β phase transition in cristobalite structure $AlPO_4$ (Phillips et al. 1990), as well as SiO_2 cristobalite (Spearing et al. 1990; Xiao et al. 1992). Line shapes can also be sensitive to very slow fluctuations in structures (Hz to kHz) such as orientational averaging and site exchange. Orientational averaging is a result of dynamical reorientation of the chemical shift anisotropy (CSA) tensor relative to the magnetic field. The rotation of water molecules in ice is one example (Wemmer 1978). Site exchange refers to an actual "hopping" of the atom between different structural environments, such as the observed alkali site (Na) exchange in a sodic nepheline (Stebbins et al. 1989). Line shape studies of this kind have been extensively used to examine orientational averaging and site exchange in organic compounds using ^1H and ^{13}C NMR (summarized in Fyfe 1983). More recently, these techniques have been applied to silicate systems, such as Na in zeolites (Janseen et al. 1989) and exchange between silicon species in silicate liquids (Farnan and Stebbins 1990).

Spin-lattice relaxation time studies measure the amount of time it takes for the nuclear spins to relax back to equilibrium after being excited by a radio-frequency pulse. This information is useful in understanding higher frequency (MHz) dynamics such as the softening of lattice vibrations. The only significant dissipation of nuclear spin energy is through stimulated emission; so for relaxation to take place, there must be some fluctuation or perturbation of the local magnetic field (and/or electric field, in the case of quadrupolar nuclei) around the nucleus at the Larmor resonance frequency, which for commonly studied nuclides is in the range of 10's to 100's of MHz. Changes in the relaxation time thus usually correspond to changes in the frequency of the local structural fluctuations. For example, relaxation time data has been useful in studying ferroelectric transitions in potassium hydrogen phosphate, and related materials, and determining the rates of motion near the critical temperature (Blinc et al. 1980) in a large number of systems.

Experimental Methods

NMR data were collected with a Varian VXR-400 spectrometer operating at ^{29}Si and ^{17}O Larmor frequencies of 79.459 and 54.219 MHz, respectively. High temperature static experiments were carried out with a home-built horizontal solenoid probe capable of temperatures greater than 1300° C (Stebbins 1991). Room temperature magic-angle spinning (MAS) experiments were carried out with a 5 mm high-speed MAS probe at a spinning speed of 10 kHz (Doty Scientific, Inc.), and high temperature MAS experiments were carried out with a 7 mm high-temperature MAS probe at spinning speeds of 2.5–3.5 kHz (Doty Scientific, Inc.). Sample temperatures for the static high temperature experiments were calibrated against the furnace control thermocouple in a separate non-NMR high-temperature run in which a thermocouple was placed inside a BN sample container filled with Al_2O_3 powder. The standard error for this calibration was ± 1.5° C. The accuracy of the sample temperature for the high temperature MAS experiments was within ± 5° C, as confirmed by the cristobalite transition temperature independently determined by differential scanning calorimetry (DSC). Chemical shifts were referenced to room temperature tetramethylsilane (TMS) for ^{29}Si and to room temperature tapwater for ^{17}O. A 97% N_2 3% H_2 mixture blanket gas was used during the static high temperature experiments on quartz to prevent oxidation of the Mo r.f. coil. For the high temperature MAS experiments on cristobalite, pure N_2 gas from liquid nitrogen boil-off was used. Experiments using the home-built probe were allowed to equilibrate for 10–30 min at each temperature step before measurements were taken, while the high temperature MAS probe was allowed to equilibrate for 5–15 min at each temperature. For both probes, observed changes with temperature were negligible for materials not undergoing structural changes (e.g. – NaCl), indicating an absence of any instrumental artifacts.

Quartz

Amethyst was chosen for these experiments (cf., Spearing and Stebbins 1989) because it was anticipated that the extremely long T_1 of pure quartz would make a detailed NMR study impossible. The amethyst sample used for the high temperature ^{29}Si NMR experiments was from a single crystal (approx. $3 \times 3 \times 3$ cm) of dark purple amethyst. A cylindrical core approximately 1 cm in diameter and 1.5 cm long was drilled perpendicular to the **c-a** axial plane. The core was oriented so that the long axis was perpendicular to the magnetic field ($\mathbf{H}_0$), and the **a**-axis made an angle of 30° with $\mathbf{H}_0$. In this orientation, maximum splitting between the

three observed resonance peaks is achieved (Spearing and Stebbins 1989). Line shape data were collected with a single $\pi/2$ excitation pulse ranging from 9–20 μs depending on the temperature. A single pulse produced an adequate signal to noise ratio (>30). Polarization times ranged from 30 min to 14 h. The ^{29}Si relaxation times were measured using the saturation-recovery method with a 16-pulse saturation comb followed by a delay τ and a single 90° detection pulse. Tau (τ) values from 1 to 5000 s were used, and an exponential fit of peak intensity vs. τ was used to calculate the relaxation time, T_1. While non-exponential relaxation of ^{29}Si has been recognized in some solids (Devreux et al. 1990; Hartman et al. 1992), our data are reasonably well fit by a single exponential decay. This was tested by fitting the decay data after removing the long delay points. If significant non-exponential behavior were present, the effect of removing the long delay points would be to significantly change the calculated T_1's, which was not observed. This test was also performed for the ^{29}Si and ^{17}O relaxation time data on cristobalite with similar results.

Cristobalite

Separate ^{17}O and ^{29}Si isotopically enriched cristobalite powders were prepared from 10% ^{17}O enriched and 57% ^{29}Si enriched amorphous SiO_2 from Cambridge Isotope Labs and Oak Ridge National Laboratory, respectively. The ^{17}O enriched cristobalite was prepared by first drying the SiO_2 under Ar gas at 1050° C for 2 h, and then heating in a welded platinum tube under Ar (to prevent ^{17}O loss) at 1600° C for 12 h. The ^{29}Si enriched sample was prepared by heating the ^{29}Si enriched amorphous SiO_2 in air at 1530° C for 8 h. Powder XRD scans from 5–60° 2θ confirm complete conversion of the amorphous SiO_2 powders to cristobalite, with no other detectable phases present. Approximately 0.105 g of $^{29}SiO_2$ and 0.48 g of $Si^{17}O_2$ cristobalite were used in the NMR experiments.

For the ^{29}Si enriched sample, ^{29}Si relaxation times were measured using the saturation-recovery method with a 16-pulse saturation comb followed by a delay τ and a single 90° detection pulse. Delay times (τ) between the saturation comb and detection pulse ranged from 1 to 2000 s. Again, one shot produced an adequate signal to noise ratio (>30).

^{17}O line shape data were collected with a $(90_x-\tau-90_y)$ solid state echo pulse sequence with a τ of 50 μs. Time domain data were digitized at a rate of 2 MHz to ensure exact locations of the echo maxima and a 170 kHz filter to increase the signal to noise ratio. ^{17}O relaxation times were measured using the saturation-recovery method described by Avagadro and Rigamonti (1973) with a 1024-pulse saturation comb. Saturation pulses were separated by 200 μs and lasted for 5.5 μs each (the solid 90° time at room T). A solid state echo was used to detect the signal for a series of delays τ following the saturation by 0.1–3000 s.

Due to the wide temperature range over which the α-β cristobalite transition can occur, differential scanning calorimetry (DSC) was used to locate the transition temperature (T_o), both upon heating and upon cooling. The DSC experiments were conducted on a Dupont Thermal Analysis 2100 DSC. Approximately 8 mg each of the ^{29}Si and ^{17}O enriched cristobalite powders were loaded into aluminum pans for analysis. The DSC scans were done under Ar gas, and calibrated against the melting points of indium (T_m= 156.61° C) and zinc (T_m=419.58° C). Two scans were done for each sample, on previously heated and unheated ^{17}O enriched samples and on a previously heated ^{29}Si sample (Table 1). A 20° C per min heating/cooling rate was used, and the transition temperature was determined by the onset (slope break) of the heat flow as a function of temperature. We observed an approximately 15° C hysteresis of T_o upon cooling for the ^{17}O enriched samples, which is consistent with previous DSC experiments on cristobalite (Hill and Roy 1958; Leadbetter and Smith 1976). The ^{29}Si enriched sample showed no hysteresis of T_o between the heating and cooling cycles. Both the ^{29}Si and ^{17}O enriched samples showed a fairly broad (10–15° C FWHM) peak in heat flow as a function of temperature at the transition suggesting that the α- and β-phases coexisted over this range, which is also consistent with previous DSC measurements. A 10° C per min heating/cooling rate scan was also carried out on the ^{29}Si enriched sample, and showed the same peak width as for the 20° C per min scans, indicating that the temperature region over which the α- and β-phases coexists is independent of heating rate. There was a small (1.5–2° C) decrease in the observed transition temperature upon heating between the two scans run on all samples. However, no change in T_o upon cooling between the two scans was observed, and there is no difference in the transition temperature for the previously heated and unheated ^{17}O cristobalite samples.

Table 1. Cristobalite α/β Inversion Temp. from DSC

Sample	T_o upon heating (°C)	T_o upon cooling (°C)
^{29}SI Cristobalite[b]	226.8	226.4
	224.9	226.4
^{17}O Cristobalite[a]	255.1	239.7
	254.2	239.7
^{17}O Cristobalite[b]	255.3	239.2
	253.7	239.3

[a] Previously unheated sample
[b] Previously heated in NMR experiment

Results

Spin-Lattice Relaxation Times

^{29}Si-Quartz. A plot of the ^{29}Si spin-lattice relaxation times (T_1) for amethyst is given in Fig. 1. These data were collected in three temperature cycles that started and ended at ambient temperature with a maximum between 800° C and 870° C for each cycle. No attempt was made to keep the temperatures strictly increasing or decreasing within each cycle. The overall pattern observed for T_1 as a function of temperature is as follows (see Fig. 1): a fairly long (3000–4000 s) T_1 is observed at ambient temperature dropping off to around 800 s at T_o, at which point there is a sharp break in the slope. Above T_o, the T_1's are constant within error at about

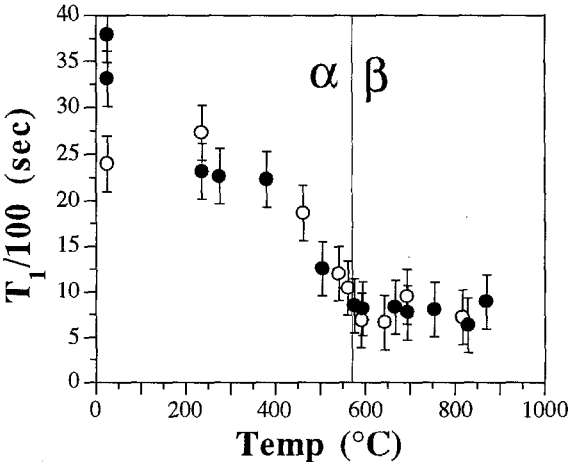

Fig. 1. ^{29}Si relaxation time vs temperature for single crystal quartz (var. amethyst). *Open circles* represent measurements taken before the iron in the amethyst was reduced by the blanket gas (see text), and *solid circles* are measurements taken after reduction

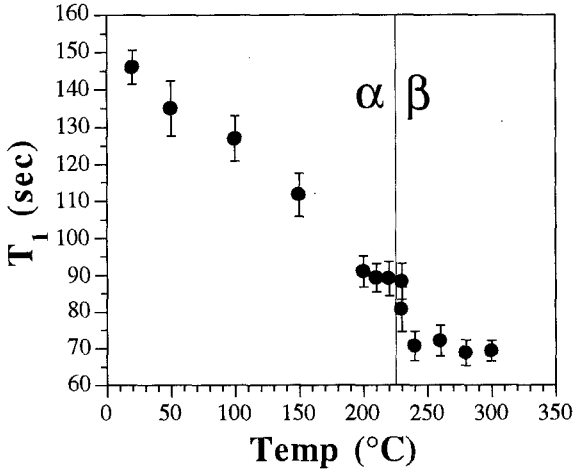

Fig. 2. ^{29}Si relaxation time (T_1) vs temperature for 57% ^{29}Si enriched cristobalite powder. α-β transition line determined from DSC scans

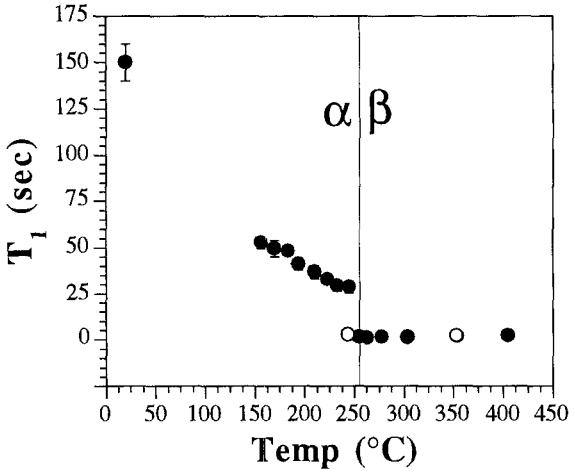

Fig. 3. ^{17}O relaxation time (T_1) vs temperature for 10% ^{17}O enriched cristobalite powder. α-β transition line determined from DSC scans. *Solid circles* are for increasing temperature, *open circles* are for decreasing temperature

800–900 s up to the maximum temperature observed (870° C).

An N_2-H_2 mixture blanket gas was used to prevent oxidation of the molybdenum r.f. coil and furnace windings. Upon removal of the amethyst sample after the first run, its color changed from the original deep purple to nearly colorless, probably due to reduction of the Fe^{4+} impurity (Cox 1977). T_1 data from this first run are plotted in Fig. 1 as open circles, and all subsequent points are plotted as filled circles. The effect of this reduction appears to have been to raise the Si T_1's by 1000–1300 s at room temperature. Above room temperature, those T_1's from the first heating cycle appear coincident within error to the measurements from subsequent heating cycles.

^{29}Si-Cristobalite. All high temperature experiments on the 57% enriched ^{29}Si cristobalite (T_1 and lineshape) were done using the Doty high temperature MAS probe. ^{29}Si T_1 data were collected for increasing temperature only. The relaxation time for cristobalite (Fig. 2) is 146 ± 4 s at ambient temperature and decrease linearly with increasing temperature to 89 ± 5 s just below the transition temperature. Above the transition, T_1 is constant within error at 70 ± 4 s. α- and β-cristobalite have different chemical shifts (as discussed below) and at 230° C both phases were present. We were thus able to measure T_1 for both simultaneously, and observed an 7 sec difference between the two at the transition: 88 ± 5 s for α-cristobalite, and 81 ± 6 s for β-cristobalite.

A similar set of T_1 measurements was also taken on a 95% enriched ^{29}Si cristobalite sample using the static high temperature probe. The results are of lower resolution than those from the high-T MAS probe (e.g., – the discontinuous jump in T_1 between the α- and β-phases is not resolvable), however the slope and intercept of the T_1 vs. temperature fits are the same within error.

^{17}O-Cristobalite. ^{17}O relaxation times for cristobalite (Fig. 3) show a similar behavior as a function of temperature relative to the ^{29}Si T_1 data for cristobalite. At ambient temperature, $T_1 = 150 \pm 10$ s, and decreases to 29 ± 3 s just below the transition, at which point there is an abrupt 1.5 order of magnitude drop in T_1 to 1.5 ± 0.2 s at T_o. Above T_o, T_1 remains nearly constant with only a slight positive slope. This jump in T_1 occurs at a temperature 15–20° C lower upon cooling, as expected from the DSC results.

Line Shapes

^{29}Si-Quartz. Spearing and Stebbins (1989) noted that for general orientations of a quartz crystal within a magnetic field, there are three ^{29}Si resonance peaks corresponding to each of the three differently oriented but crystallographically equivalent SiO_4 tetrahedra in the unit cell. As the crystal is rotated, these resonance peaks map out the chemical shift anisotropies (CSA) of the

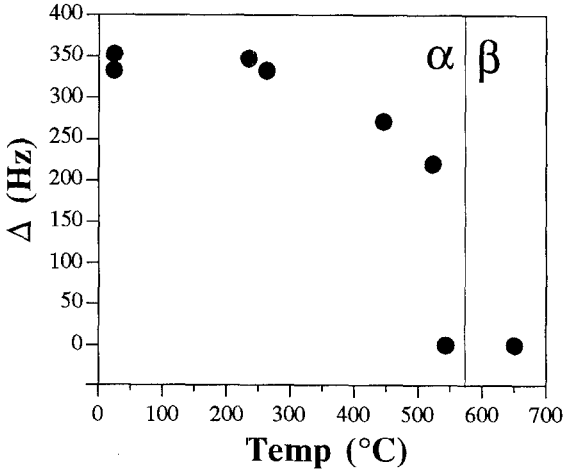

Fig. 4. Peak separation (Δ) between the two outside peaks in the static ^{29}Si spectrum of a single crystal of quartz (oriented as described in text) as a function of temperature

silicon atoms, which are identical, but differ in orientations. For the specific orientation described in the experimental section, we observe the same three peaks as described earlier, although somewhat broadened due to the increased field inhomogeneity over the larger coil and sample volume used in the high-temperature probe. With increasing temperature, the peaks move closer to one another such that at T_o (573° C) and above, only one peak is observed. The distance between the two outside peaks plotted as a function of temperature (Fig. 4) shows that this coalescence begins to occur at least 150° C below the transition temperature. This is also the point at which the heat capacity (Ghiorso et al. 1979) begins to show a marked premonitory rise over that expected for a simple vibrational heat capacity. With increasing temperature, the orientational distinction among the three Si sites in the quartz unit cell decreases either because of a static or time-averaged reduction in the CSA. Above the transition only a single Si peak is observed.

In addition to a coalescence of the three peaks, we also observe an overall shift of the peak positions toward lower frequency up to T_o, above which the chemical shift is relatively constant. X-ray refinements of the quartz structure show an increase in the mean Si-O-Si bond angle with increasing temperature (e.g. – Kihara 1990). This is consistent with correlations of ^{29}Si chemical shifts and mean Si-O-Si angle (Engelhardt and Michel 1987), which predict that the chemical shift should decrease with increasing Si-O-Si bond angle. Fig. 5 shows the experimental peak positions as a function of temperature. Also plotted are the isotropic chemical shifts as predicted by the correlation of Engelhardt and Radeglia (1984) using Si-O-Si angles from the XRD refinement by Kihara (1990). Though it is not possible to calculate the isotropic chemical shift based on a single crystal spectrum from one orientation, we observe that the experimental peaks follow the same trend as the calculated

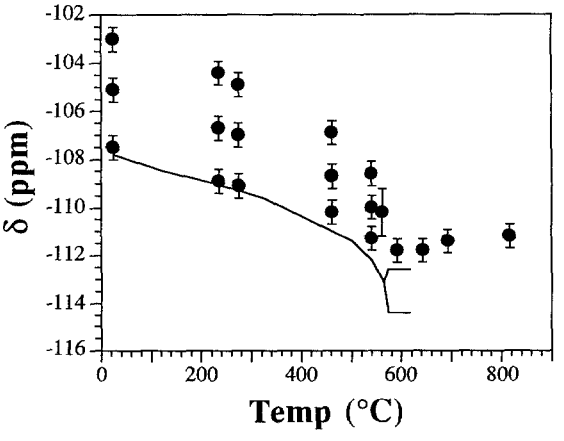

Fig. 5. ^{29}Si chemical shift vs temperature for single crystal quartz with orientation $C \wedge B_o = 30°$. *Points* are experimental peak positions, while the *solid line* is the isotropic chemical shift calculated from the Si-O-Si bond angles determined from x-ray by Kihara (1990). The two lines above the transition temperature (573° C) represent a split-atom refinement (*upper line*) and a normal refinement (*lower line*) for the oxygen sites.

isotropic chemical shift and appear to be consistent with the split-atom refinement for β-quartz (Kihara 1990).

Since the absolute orientation of the CSA tensor relative to the crystallographic axes has been determined (Spearing and Stebbins 1989), any changes in the peak positions or line shapes can be related to orientational or shape changes of the tetrahedra. An exception to this is the 180° rotation required for the Dauphiné twin. As discussed previously, β-quartz can be thought of as a space and/or time average of the two Dauphiné twin related configurations, α_1 and α_2. Due to symmetry constraints, the α_1 and α_2 configurations will give identical NMR spectra. The 180° rotation imposed upon the tetrahedra by the twin, and hence the silicon CSA tensor, causes the CSA to rotate such that those sites giving rise to the peak at −102.7 ppm in the room temperature spectra are exchanged with those at the −107.7 ppm resonance. The sites giving rise to the central −105.1 ppm line are unaffected by the rotation (that is, a 180° rotation of the CSA for those spins produces the same shift). Thus, the two Dauphiné twin related configurations will have identical spectra. A similar argument can be applied to the Brazil twin as well, which relates the left and right handed enantiomorphs. Thus, the presence of Dauphiné and/or Brazil twin in quartz should have no effect on the line shape relative to an untwinned sample.

The observed coalescence of peaks could be caused by either a rotation in the static orientations of the tetrahedra toward those in the ideal high T structure, or by dynamic averaging. In the former case, the coalescence of the peaks would be caused by the positions of the two outer resonances moving closer to and eventually coinciding with the central resonance as each tetrahedron (and the associated CSA tensor) rotates to the same orientation. The effect of this on the NMR spectrum can be investigated by simulating the temperature dependent spectra as superpositions of three Lorentzian lines, with widths ($1/T_2$, where T_2 = spin-spin relaxation time) determined from the room temperature spectrum. The higher temperature spectra can be adequately modeled in this manner with only a modest amount of line broadening added (~50 Hz), which could be attributed to increasing field inhomogeneity. The observed changes in lineshape could also be equally well fit by simulation of a dynamical exchange between the two outside peaks, which would result if the tetrahedra were flipping between the dauphiné twin orientations. When dynamic averaging occurs, two effects are predicted (Anderson 1954): as the rate of exchange increases, lines move together and broaden before collapsing to a single narrow line.

Dynamic averaging calculations are based on writing the equation of motion of the spin magnetization in terms of the frequencies and relaxation times of the spins at specific sites and an exchange matrix which describes the probability of a transition between sites (Abragam 1961, p 447). The exchange matrix is constructed to describe a particular model of reorientation or diffusional exchange. In the present case, we are modelling the exchange between different magnetic environments caused

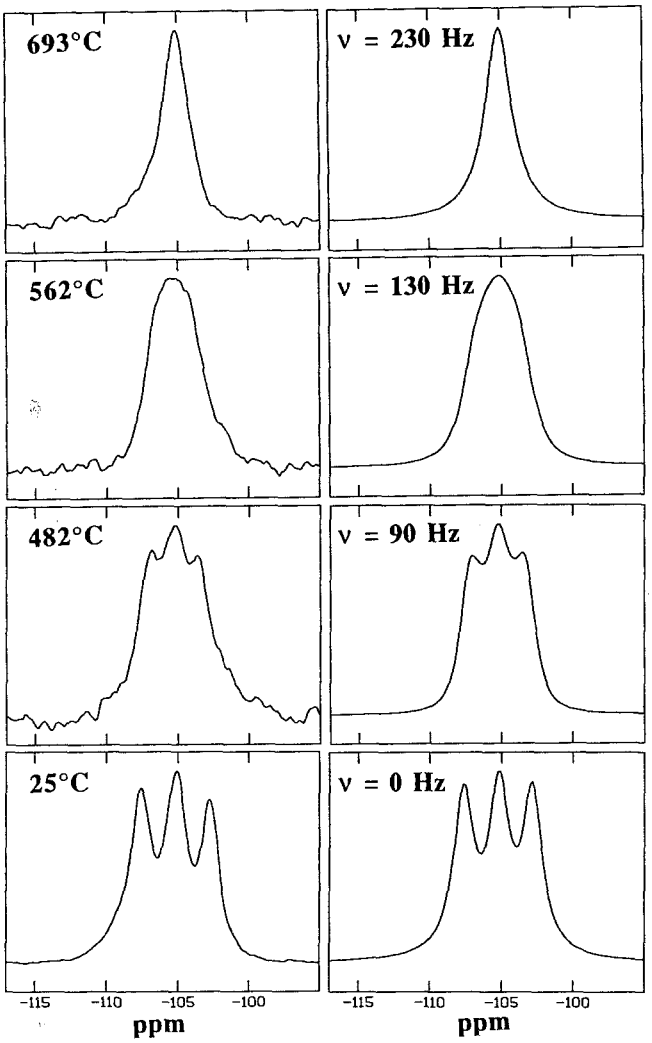

Fig. 6. Experimental (*left*) and simulated (*right*) ^{29}Si spectra for single crystal quartz. The modeled exchange frequencies between the two outside peaks are given with the simulated spectra. Peak positions for above ambient spectra have been adjusted such that the middle peaks line up with the middle peak of the ambient temperature spectrum

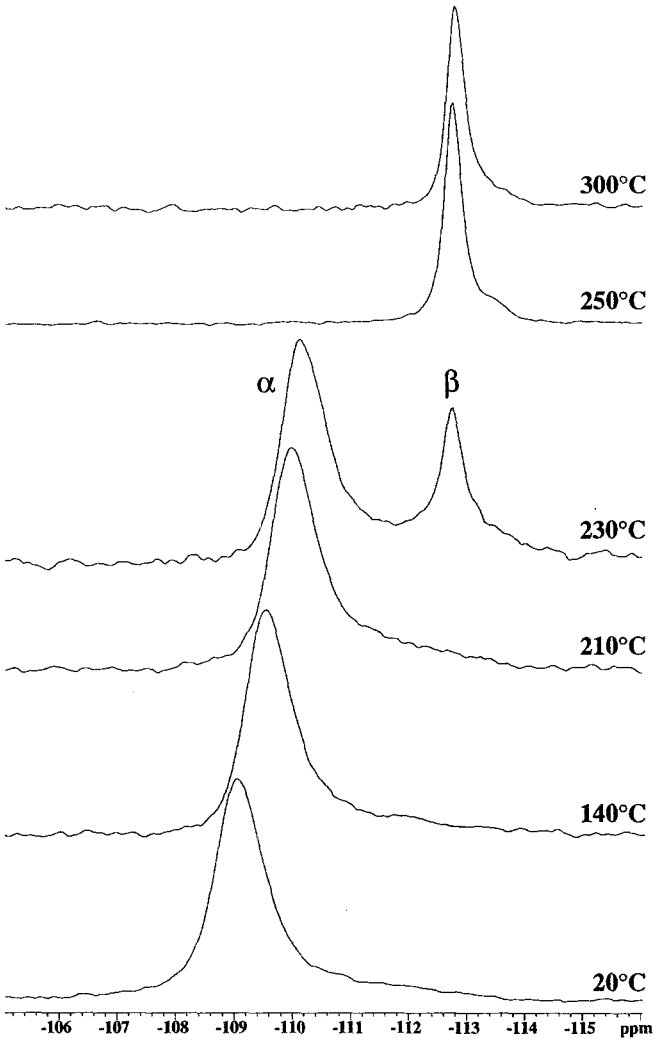

Fig. 7. High temperature ^{29}Si MAS spectra for 57% enriched cristobalite powder. Peaks for both α- and β-cristobalite are present in the spectrum from 230° C

by a slight rotation of the tetrahedra (and hence the CSA tensor), and no bond breaking or diffusion is required. The starting point was to simulate the room temperature spectrum. The only parameters used were the peak positions and peak widths ($1/T_2$). The higher temperature spectra were then fit "by eye" allowing only the exchange between the two outside peaks because of the effects of α_1–α_2 domain symmetry noted above. (This model is further supported by the fact that the spectra could not be fit if an exchange between all three peaks is used.) A slight increase in T_2 was also allowed (0.015 sec at ambient, up to 0.07 sec for all spectra above 450° C), which is consistent with the fact that T_2 generally increases with increasing temperature. The actual and simulated spectra for four temperatures are shown in Fig. 6. At temperatures below which the line shape is unaffected by dynamics ($T < \sim 300°$ C), this approach can only give the maximum exchange rate. Similarly, above the point where the line width is reduced so much that it is dominated by other effects such as magnetic field heterogeneity ($T > \sim 700°$ C), this model can only estimate a minimum rate.

^{29}Si-Cristobalite. A single peak centered at a frequency of −109.1 ppm is observed for the room temperature ^{29}Si MAS spectrum of cristobalite, which is consistent with previously reported results of −108.5 ppm (Smith and Blackwell 1983), −109.9 ppm (Lippmaa et al. 1980), and −108.6 ppm (Xiao et al. 1992). The peak width is about halfway between most ordered and disordered cristobalite samples of Xiao et al. (1992). The peak position decreases in frequency with increasing temperature to −110.0 ppm just below T_o (Fig. 7). At T_o the chemical shift jumps from −110.2 ppm in the α-phase to −112.7 ppm in the β-phase, and over an approximately 20° range above T_o, peaks for both α- and β-cristobalite are present. Above the transition, the peak position for β-cristobalite appears to remain constant at −112.7 ppm. Coming down in temperature, the onset of the transition occurs at the same temperature as for heating. There is a hysteresis, however, for the range

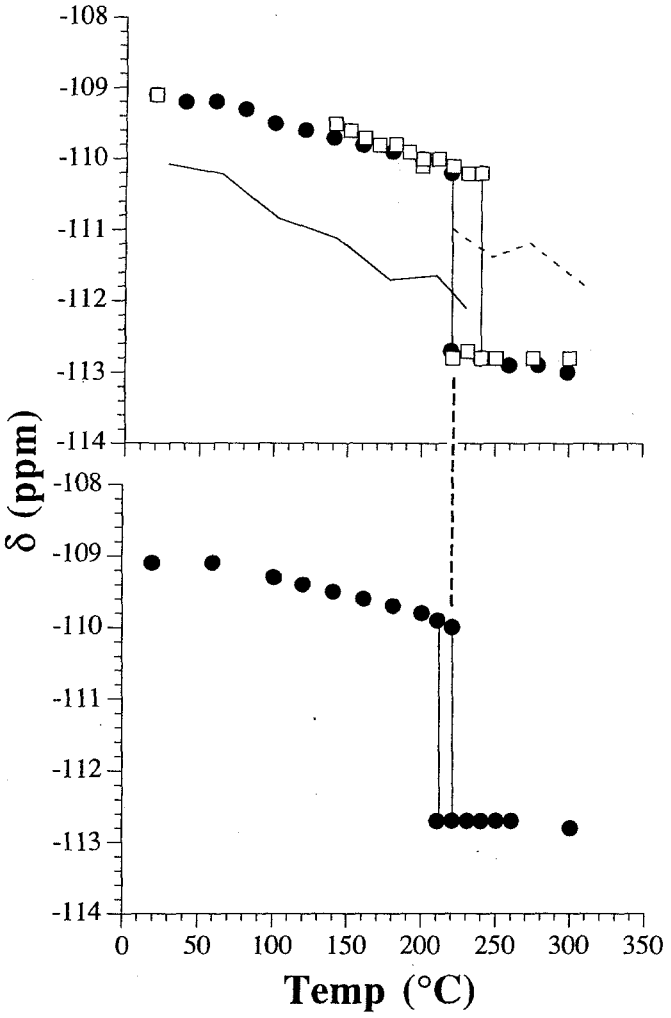

Fig. 8. ^{29}Si chemical shift vs. temperature for 57% enriched cristobalite powder. *Top plot* is for temperature increasing, *bottom plot* is for temperature decreasing. *Circles* and *squares* in top plot are for two separate runs. Note that the onset temperature is the same for both temperature increasing and decreasing, but there is still a hysteresis in the region where α- and β-phases coexist. *Lines* in the upper plot are the isotropic chemical shifts calculated from the Si-O-Si bond angles determined from x-ray by Peacor (1973). *Solid line* is based on α-cristobalite angles, while *dashed line* is from β-cristobalite angles

over which the α- and β-phases coexist. Linewidths are constant at 65 ± 2 Hz below T_o, but drop to 20 ± 0.5 Hz across the transition.

Based on correlations of ^{29}Si chemical shifts with Si-O-Si angles (summarized in Engelhardt and Michel 1987), which show that chemical shift decreases with increasing angle, the above results imply a decreasing angle with increasing temperature below the transition, and a temperature independent Si-O-Si angle above the transition. Calculated chemical shifts based on Si-O-Si angles determined from single crystal high temperature x-ray diffraction (Peacor 1973), and the correlations of Engelhardt and Radeglia (1984), show a similar trend (Fig. 8). However, the slope as determined by XRD ($m = -0.0100 \pm 0.0008$) is about twice that as observed by NMR ($m = -0.0051 \pm 0.0002$). Calculated chemical shifts based on other correlations (Smith and Blackwell 1983; Radeglia and Engelhardt 1985) show the same slope within error. Above the transition, the Si-O-Si angle observed from x-ray refinement correlates to a much higher chemical shift for β-cristobalite than that observed. As discussed below, the reasons for these discrepancies are probably a rocking motion of the oxygen out of the Si-O-Si plane in α-cristobalite and motional averaging in β-cristobalite.

^{17}O-Cristobalite. Although more difficult to simulate than single-crystal spin 1/2 spectra, a great deal of information about site symmetry, local environment, and dynamics can be obtained from static powder spectra for quadrupolar nuclei such as ^{17}O (spin $I = 5/2$). The quadrupolar interaction is usually described by the quadrupolar coupling constant (QCC), which for a given nuclide is a measure of the electric field gradient (EFG) at the nucleus, and the quadrupolar asymmetry parameter (η) which is a measure of the deviation of the EFG from axial symmetry (Kirkpatrick 1988). The average chemical shift, the CSA, EFG, η, and the relative orientations of the EFG and CSA tensors all effect the line shape of static powder patterns and must be taken into account in simulations. However, data on some of these variables can be more simply obtained from MAS spectra in which the CSA is averaged.

For cristobalite, we examined both ambient to high temperature ^{17}O static powder patterns and ambient MAS spectra. We began by fitting the MAS spectrum to determine the EFG, η, and isotropic chemical shift (δ_{iso}) using a computer program based on the methods outlined by Müller (1982). Results are shown in Fig. 9, with $QCC = 5.3 \pm 0.1$ MHz, $\eta = 0.125 \pm 0.005$, and $\delta_{iso} = 40 \pm 2$ ppm. This value for the QCC is identical to that reported by Timken et al. (1986a) for ^{17}O MAS spectra. However, Timken et al. (1986a) report that $\eta = 0$ for cristobalite yet state that $\eta = 0.1$ for oxygen in most Si-O-Si linkages. Clearly, the latter is the case for cristobalite. Using these constraints, the principle components of the CSA tensor (σ_{11}, σ_{22}, σ_{33}) were then obtained by fitting the static powder spectrum (Narita et al. 1966). Assuming that the principal axes of the EFG and CSA coincide, we obtain $\sigma_{11} = 60$, $\sigma_{22} = 60$, and $\sigma_{33} = -10$ ppm ($\pm$ 5 ppm for all values). No better fit could be obtained by allowing the angle between the principle axes of the CSA and EFG tensors to vary. It was also not possible

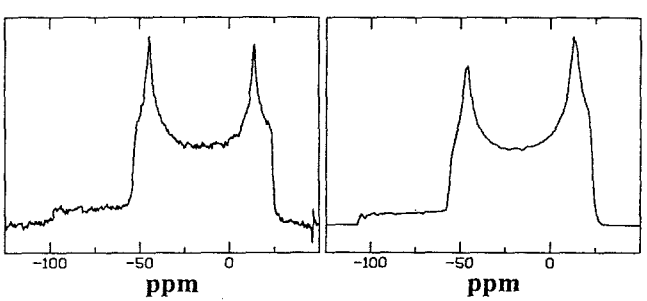

Fig. 9. Experimental (*left*) and simulated (*right*) room temperature ^{17}O MAS powder spectra for cristobalite

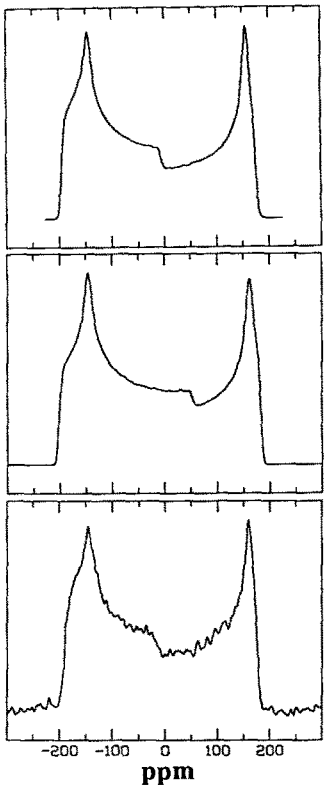

Fig. 10. Experimental (*bottom*) and two simulated room temperature ^{17}O static powder spectra. Middle simulation was done with the CSA = 0, while the top simulation accounts for both the CSA and quadrupolar parameters (EFG and η)

to fit the static powder spectra considering only the quadrupolar and isotropic chemical shift terms (Fig. 10). The separation between the horns and shoulder width could be fit adequately since they are controlled by the EFG and η. However, the position of the singularity in the center of the spectrum could not lined up between the simulated and real spectra (note that in the real spectrum the central singularity occurs at about 0 ppm, while in the simulation with it occurs at about 75 ppm). In addition, the EFG determined for the static spectra considering an isotropic chemical shift was 5.7 MHz, which does not agree with the value of 5.3 MHz as determined from the MAS fit. Based on the values obtained for the principle axes of the CSA, we calculate the isotropic chemical shift $\delta_{iso} = 36.7$ ppm (± 5 ppm), which is in agreement with the value determined from the MAS fit. This is somewhat less than the previously reported value of 46 ppm for static spectra (Timken et al. 1986a) and 44 ppm for MAS spectra (Timken et al. 1986b). This discrepancy may be due to our inclusion of a non-zero asymmetry parameter (η).

All above-ambient spectra could be simulated by varying only the asymmetry parameter (η), retaining the room temperature EFG and CSA values. Since the spectra could be modeled at high temperature without varying the CSA, this implies that the rotation of the oxygens is constrained along a principle axis of the CSA. Thus, there is no averaging of the CSA, and the motion cannot be modeled by random diffusion. The actual and simulated spectra for four temperatures are show in Fig. 11. We observe that with increasing temperature there is a decrease in the asymmetry parameter, such that at 15–20° C below the α-β transition η is less than 0.04,

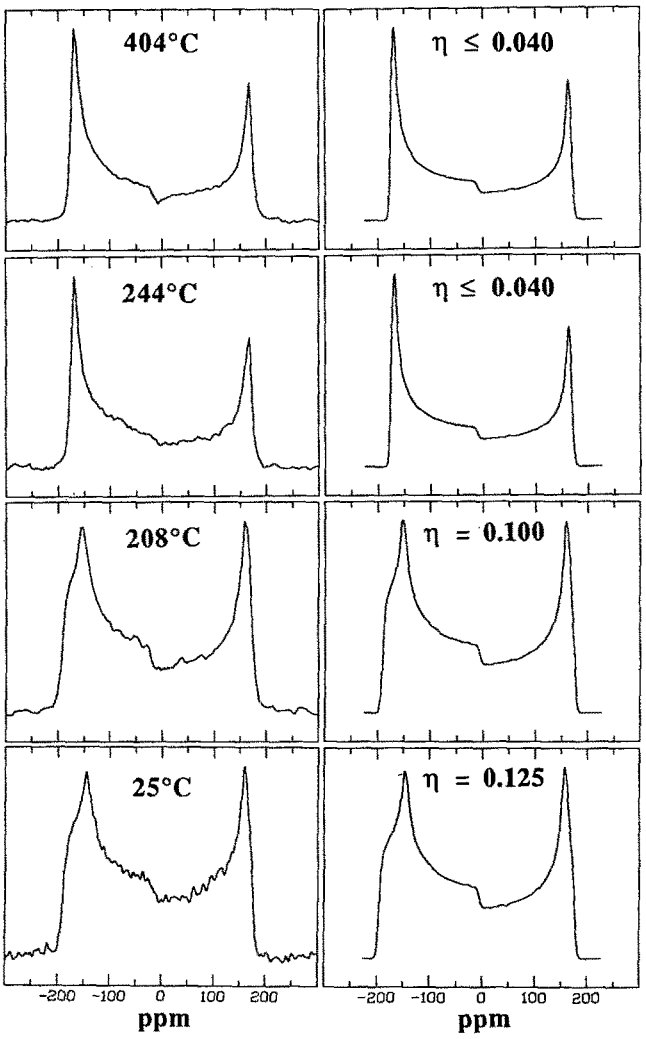

Fig. 11. Experimental (*left*) and simulated (*right*) static ^{17}O powder spectra for cristobalite. The asymmetry parameters (η) as determined from the fit are given with the simulated spectra. Values of $\eta \leq 0.04$ are indistinguishable from $\eta = 0$. Recycle delays of 30 s were used to ensure that the lineshapes were not dominated by the faster relaxing β-phase

which is the minimum value that can be distinguished from zero for our data. All spectra above this temperature are identical, again with $\eta \cong 0$. Thus, with increasing temperature the oxygen site in cristobalite becomes more axially symmetrical.

As for quartz, the observed line shape change could be caused either by a static increase in local symmetry, or by dynamical averaging. If the latter is the case, our results are consistent with a jumping of the oxygen among the positions suggested by XRD, resulting in a time average cylindrical symmetry for the site. In the rapid motion limit, the jump frequency should be greater than the linewidth (20 KHz).

Analysis and Discussion

Quartz

Analysis and modeling of the ^{29}Si line shapes for quartz has shown that with increasing temperature, the three

magnetically different silicon sites in quartz become similar. One interpretation of this is an exchange or oscillation between the α_1 and α_2 configurations below the transition temperature, which is how we have modeled it here, although a static model fits the data equally as well. Similarly, the ^{17}O line shapes from cristobalite show that the EFG at the oxygen site becomes more axially symmetric with increasing temperature, and one interpretation is that the oxygens are rotating in an annulus that circles the Si-Si axis in the $Fd\bar{3}m$ structure. However, from line shape studies alone one cannot necessarily distinguish between static and dynamic disorder. The relaxation time experiments provide additional evidence that suggests in both quartz and cristobalite that the high temperature structures as observed by x-ray are probably dynamic averages of low-temperature domains, and that there may also be considerable motion of the SiO_4 tetrahedra below T_o.

For quartz, we have already noted that T_1 decreases up to T_o, and remains relatively constant above T_o. (There is some suggestion in the T_1 vs temperature data for quartz, Fig. 1, that T_1 begins to level off at around 200° C, and then drop off again near 400° C. This would fit nicely with the observations that at about 150° C below the transition, the peaks in the ^{29}Si single crystal spectrum begin to coalesce, and the measured heat capacity shows a marked premonitory rise over that expected for simple vibrational heat capacity. However, the leveling off and subsequent decrease in T_1 is on the same scale as the scatter in the data. The matter is further complicated by the reduction of the iron in the amethyst.) This is very different behavior from what has been observed in many other displacive phase transitions. In most cases, T_1 decreases with increasing temperature up to the phase transition, and then increases with increasing temperature above the transition (Rigamonti 1984). The relaxation time in these cases is usually related to a vibrational soft mode that hardens above the transition temperature, and this behavior has been observed for both spin 1/2 (e.g. – ^{31}P in CsD_2PO_4 and KD_2PO_4, Blinc et al. 1980; Blinc et al. 1977) and quadrupolar nuclei (e.g. – ^{23}Na in $NaNbO_3$, Avogadro et al. 1974). In most experiments of this type the relaxation mechanism is usually well known (e.g. – dipolar-dipolar coupling, quadrupolar, or CSA coupling) and hence the T_1 vs. temperature behavior can be accurately modeled. However, spin-lattice relaxation of ^{29}Si in solids is not well understood in detail. Given the very small CSA for quartz (Spearing and Stebbins 1989) it is highly unlikely that CSA coupling can be responsible for the observed relaxation times (Liu et al. 1987; Harris 1983), even if the averaging was taking place over the whole of the CSA (an extreme assumption given symmetry constraints in the crystal). It is thus likely that coupling to the large local magnetic fields generated by paramagnetic ions must make a significant contribution to the relaxation, as has often been suggested previously for silicates (Engelhardt and Michel 1987).

The problem is thus to separate changes in T_1 caused by "background effects" (i.e. – changes in the correlation time of the electrons in the paramagnetics with increasing temperature that are present in the absence of any phase transition), with the effects on T_1 caused by fluctuations associated with the phase transition. Tse and Lowe (1968) have shown that there is a strong temperature effect on the electron correlation time (τ_c) at temperatures well below the Debye temperature (Θ_D) for a given substance ($\tau_c \propto T^{-7}$), and that this effect is independent of how the nuclear spins are coupled to the paramagnetics. At temperatures close to or greater than Θ_D, this effect levels off to a T^{-2} dependence of τ_c. This change in correlation time has been shown to have a profound effect on the relaxation time of quadrupolar nuclei that are coupled to the paramagnetic centers (Weber 1963) via the anharmonic Raman phonon process (Van Kranendonk and Walker 1967). However, the change in T_1 with temperature due to this process is a continuous function, and thus cannot be responsible for the discontinuity observed in the ^{17}O T_1's for cristobalite. For spin 1/2 nuclei, when the spin energy is transmitted via spin diffusion to paramagnetic centers, Tse and Lowe (1968) reported a much smaller correlation between the electron correlation time and T_1 ($T_1 \propto \tau_c^{1/4}$). Thus, for the case of ^{29}Si relaxation in quartz and cristobalite in this study, where the temperature range is close to or above the Debye temperature and spin diffusion is the likely mechanism for relaxation, we expect a relatively minor contribution from the temperature dependence of the electron τ_c to the observed drop in T_1 with increasing temperature. Among the only other studies ever made of ^{29}Si relaxation at high temperature are those of silicate glasses of Liu et al. (1987) and Farnan and Stebbins (1990), which were doped with paramagnetic impurities to reduce T_1. Here, increasing temperature had very little effect on T_1, until the dramatic dynamical changes at the glass transition began. These results suggest that simple local vibrations or changes in the electron τ_c cannot cause the large temperature effect on T_1 noted here. Crystalline lattice dynamics can potentially, however, contribute other, poorly known relaxation mechanisms that are not present in a glass.

Despite the fact that the exact nature of the relaxation mechanism for ^{29}Si is unclear, we can still use relaxation time measurements to extract some information about the dynamics in the structure. The full expression for T_1 can be broken into the products of two terms: one a function of the coupling between the nucleus and surrounding dipoles ("coupling term"), and the other a function of any fluctuations occurring in the structure ("dynamic term"), (Abragam 1961). The dynamic term is generally the one that has the largest dependence on temperature. Thus, though we may not quantitatively know the exact nature of the coupling term (i.e. – the role that the paramagnetics play in the relaxation), a plot of T_1 vs. temperature will give information about the effects of the *dynamics* of the relaxation since only the dynamical term has a strong temperature dependence.

It is doubtful that the very slow fluctuations in quartz (about 230 Hz) as modeled from the lineshape study could be directly responsible for a decrease in the relaxation time. There must be a significant tail of the spectral

density curve at the Larmor frequency (ν_L) to affect relaxation, yet ν_L is many orders of magnitude (79.459 MHz for ^{29}Si) above the fluctuation frequency. We note that even a low frequency hopping motion, if abrupt, has significant high frequency components. In addition, as discussed previously, there is a softening of the 207 cm^{-1} vibrational mode which begins about 200° C below the transition (Raman and Nedungadi 1940) and has been attributed as the lattice vibration fundamentally associated with the α-β phase transition (Shapiro et al. 1967). The behavior of this mode with increasing temperature is remarkably similar to our T_1 data (see Fig. 1. in Höchli and Scott 1971) and has also been found not to go to zero at T_0 (Shapiro et al. 1967). In addition, a "residual" forbidden A_1-type Raman mode persists into the β-phase (Shapiro et al. 1967). The quartz T_1 data are in agreement with these studies; the decrease in T_1 could be attributed to the softening of the 207 cm^{-1} mode, and the fact that it is constant above T_0 suggests that the fluctuation causing the relaxation is still present above the transition. Thus, although the slow fluctuation predicted from the lineshape simulations may be too slow themselves to significantly contribute to relaxation, they may be related in some manner to higher frequency soft mode vibrations.

One way to model the fluctuation of the silicon tetrahedra from one Dauphiné twin related configuration to the other is to assume that they must first pass over a potential energy barrier of some kind and through an intermediate state, and that this can only happen at a certain rate dependent on the temperature. From a structural standpoint, this is not an unreasonable assumption if the intermediate state is the average β-quartz position and if this configuration is not energetically favorable (which it is not at temperatures below the phase transition). The apparent activation energy for this process can be estimated from the slope of an Arrhenius plot. Figure 12 shows such a plot of both the ^{29}Si relaxation times for quartz and the exchange times ($1/\nu_{exch}$) as derived from the line shape simulations. Near the transition temperature both show the same slope

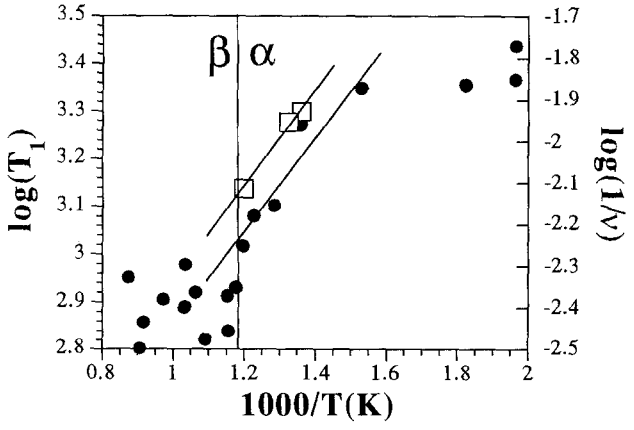

Fig. 12. Log(T_1) for ^{29}Si in quartz (*filled circles*), and log(1/ν) as determined from fitting the ^{29}Si spectra in quartz (*open squares*) vs. 1/temperature. Vertical scales have been adjusted so that the curves coincide

[∂ ln(time)/∂(temperature)] within error: 2800 ± 500, giving an activation energy of 23 ± 4 kJ/mol. The similarity of the slopes for the two processes seems too good to be fortuitous, and thus may support the hypothesis that the motion that causes the coalescence of the peaks in the ^{29}Si lineshape is also responsible, at least in part, for the decrease in T_1.

Two possible types of dynamical models are outlined here based on those suggested by Liebau and Böhm (1982), which describe the behavior of the potential energy surface.

(i) The SiO_4 tetrahedra begin to oscillate within (but not between) the two wells of a double-minima potential. If the α_1–α_2 potential wells are anharmonic with steep sides away from one another and a shallower potential between each other, then with increasing vibrational energy the mean positions of the tetrahedra will move toward one another. The transition is therefore marked by the temperature at which the tetrahedra have enough energy to hop over the potential barrier separating the α_1 and α_2 configurations. In this model, there is no hopping between the α_1 and α_2 configurations below the transition temperature, only above.

(ii) Alternatively, the changes observed in the line shape up to T_0 could be caused by oscillations of the SiO_4 tetrahedra *between* the α_1 and α_2 configurations. That is, there is some "flip-flopping" of the tetrahedra between the α_1 and α_2 configurations *below* the transition temperature. If the frequency of this oscillation is greater than the frequency separation of the peaks, then the three peaks will be averaged to one. However, if the frequency of the oscillation is less than the frequency separation of the peaks, then there will be a broadening and shift of the peaks toward one another.

Both models provide a structural mechanism for the observed drop in T_1: vibration of the tetrahedra, either within the α_1 and α_2 potential wells, or between them. However, the first model is inconsistent with the appearance and mobility of the dauphiné twin microdomains below T_0 as observed by TEM (van Tendeloo et al. 1976; Heaney and Veblen 1991). The occurrence of such microdomains requires that there be a flipping of the quartz structure between the α_1 and α_2 configurations below T_0, which supports the second model. This is also consistent with the existence of the incommensurate phase in quartz. Below T_0, the flipping between the α_1 and α_2 configurations would have to be correlated over a long scale or the averaging would be observed in the NMR spectra. With increasing temperature, the correlation length decreases, and the incommensurate phase is reached when the correlation length is of the same order as several unit cell lengths.

The transition mechanism can be further explored through theoretical estimates of the energetics of local structural perturbations. Gibbs (1982) and Navrotsky et al. (1985) have predicted potential energy surfaces for linked SiO_4 tetrahedra as a function of the Si-O-Si bond angle and bridging bond length d(Si-O) based on *ab initio* calculations of the disilisic acid ($H_6Si_2O_7$) molecule. The bond angles and bridging bond lengths of the

silica polymorphs plot along the minimum in the calculated potential energy surface for disilisic acid, suggesting that it is a reasonable approximation for the crystalline phases of silica as well. Based on their calculations, we find that the split-atom refinement for β-quartz (Kihara 1990) gives the maximum difference in energy between the two possible oxygen positions: 7.5–8.0 kJ/mol. If the average ideal β-quartz is used instead, then the difference between the α- and β-configuration is much smaller (<2 kJ/mol). In addition, the chemical shift trend of the peaks with increasing temperature (Fig. 5) is more consistent with the split-atom refinement for β-quartz. There is a larger decrease in the calculated chemical shift at the transitions if the average β-positions for the oxygens are used relative to the split-atom model which does not appear to be present in the peak position data. The energy determined from the Arrhenius plot is about three to four times that determined from the potential energy surface calculated from disilisic acid. However, this is still a fairly good agreement given that one would expect a greater amount of energy to bend or lengthen a bond in a network silicate relative to isolated tetrahedra, as in the disilisic acid, since considerable cooperative motion would be required in the solid. Thus, the rate of flipping between the α_1 and α_2 configurations can be modeled as an activated process with the intermediate state being the average β-quartz position, and that the energy potential between the two configurations is on the order of 20 kJ/mol. This flipping appears to be tied to the relaxation mechanism, exists at low frequencies below the transition, and persists above the transition, implying that the β-quartz structure exists only as a dynamical average of the Dauphiné twin related configurations.

Cristobalite

From the ^{17}O lineshape analysis, we know that the oxygen site becomes more axially symmetric with increasing temperature and this could be due to either a static or dynamic disorder of the oxygens around the ideal C9 position. Relaxation times for both ^{29}Si and ^{17}O, however, support the hypothesis of a dynamic transition producing a β-phase that is a space and time average of twin-domains, as suggested by Hatch and Ghose (1991). The effect of temperature on the ^{29}Si T_1 is very similar to that of quartz: T_1 decreases up to the transition, and then remains constant above the transition. Applying similar arguments to the ^{29}Si relaxation in cristobalite as were used for quartz, we can say that whatever the relaxation mechanism, it is tied to the dynamics of the transition (given the drop off and break in slope).

The compelling evidence for a dynamically averaged structure for β-cristobalite comes from the ^{17}O relaxation data. The observed 1.5 order of magnitude drop in T_1 at the transition cannot be caused by just a simple rotation of the tetrahedra to the high temperature orientations, nor due to an abrupt change in the electron correlation time as discussed previously. Although we do not quantitatively know what the relaxation mechanism is, as with quartz, it must be tied to some oscillatory motion. For ^{17}O, the relaxation cannot be due to a change in the principle component of the EFG or CSA, since the lineshapes can be modeled without varying these parameters. Thus, the relaxation and lineshape changes may be due to a hopping of the oxygens among the six 96(h) sites, which comprise the twins in low cristobalite. An ^{27}Al and ^{31}P lineshape analysis of the α-β cristobalite transition in isostructural $AlPO_4$ by Phillips et al. (1990) led to much the same conclusion about the nature of the transition.

Assuming that the α-β cristobalite transition can also be modeled where the hopping rate is an activated process, Arrhenius plots were made for the ^{29}Si and ^{17}O cristobalite T_1 data (Figs. 13, 14). Activation energies as determined from the slopes of points below T_0 are 4 ± 2 kJ/mol for ^{29}Si and 9 ± 4 kJ/mol for ^{17}O. Within experimental error, these energies are the same. Plotting the bond angles and distances for α- and β-cristobalite on Gibbs' (1982) potential energy surface for disilisic acid, we find that the greatest difference in energy is between the α- and C9 β-configurations: ~7.5 kJ/mol.

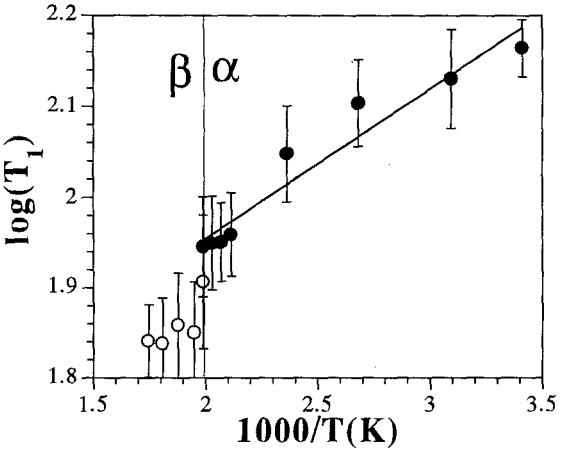

Fig. 13. Log(T_1) vs 1/Temp for ^{29}Si in 57% enriched cristobalite powder. α-β transition line determined from DSC scans

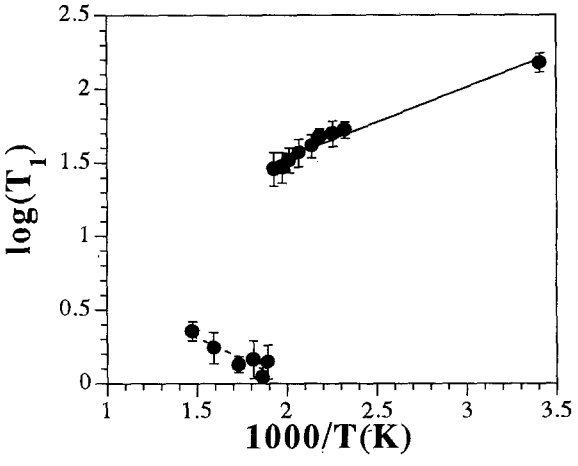

Fig. 14. Log(T_1) vs 1/Temp for ^{17}O in 10% enriched cristobalite powder

Although these energies are similar, the average β-cristobalite positions for the oxygens is probably not a good candidate for the rate limiting step required for an Arrhenius approximation. Unlike quartz, in order for the tetrahedra to rotate from one twin orientation to another they do not need to pass through the average β-positions. Rather, the oxygens rotate in a ring about the C9 position (Welberry et al. 1989). The potential barrier that must be overcome is probably the energy required for an oxygen to move from one of the twin related sites to any of the others around the annulus, rather than the mean β-position.

Further evidence supporting the dynamic nature of β-cristobalite comes from the ^{29}Si chemical shift data. As mentioned in the 'Results' section, the chemical shift vs. temperature data follow a trend similar to that predicted by the Si-O-Si angles as derived from the mean atomic position determined by XRD below T_o, although the slope predicted by XRD is about twice that observed by NMR. In a neutron powder diffraction study of low cristobalite from 10 to 473 K, Pluth et al. (1984) suggested that a rocking motion of the oxygen out of the average Si-O-Si plane could lead to a real Si-O-Si angle that is smaller than that calculated from the mean atomic positions. They concluded that accounting for this motion could reduce the calculated angle from 150.0° to 146.7° at 230° C. Thus, the observed decrease in chemical shift is probably due to a real increase in the Si-O-Si angle, while the angle as determined by XRD may be artificially greater due to an increase in rocking motion of the oxygens.

The 3 ppm drop in chemical shift across the transition does, however, suggest a real change in the Si-O-Si angle between α- and β-cristobalite, and also suggests a significant first-order character to the transition. A similar shift of −2.5 ppm was also observed in ^{27}Al and ^{31}P MAS spectra of the cristobalite phase of $AlPO_4$ across its α-β phase transition (Phillips et al. 1990). The ^{29}Si chemical shift that we have observed for β-cristobalite is also not entirely consistent with the Si-O-Si angle derived from XRD data, again probably due to rocking motion of the tetrahedra. This is further supported by the decrease in the linewidths from 65 Hz for α-cristobalite to 20 Hz for β-cristobalite, and a similar high temperature ^{29}Si MAS study of cristobalite (Xiao et al. 1992).

Thus, the structure of β-cristobalite can be represented in much the same way as β-quartz: it is a dynamical average of twin related low-temperature configurations, and this flipping between the twin related domains begins well below the transition temperature.

Conclusions

Based on ^{29}Si line shape and relaxation time data for quartz, and ^{29}Si and ^{17}O line shape and relaxation time data for cristobalite, we conclude that significant rotation of the tetrahedra between twin-related orientations occurs below the α-β transition temperature. For quartz, this rotation is probably between the α_1 and α_2 Dauphiné twins, and for cristobalite it is between the twelve twins. This exchange between the different twin orientations continues well above the transition temperature, and the β-phases are best described as a space and time average of the α-phase twin domains. Simulation of the high-T ^{29}Si single crystal spectra for quartz gives a minimum exchange frequency of 230 Hz at the transition (573° C). Assuming that the rate of this exchange can be modeled as an process with the average β-position as the rate limiting step, we find that the exchange rate and the ^{29}Si relaxation time for quartz, when plotted vs temperature on an Arrhenus plot, give the same slope within error below the transition. This implies that the slow oscillations of the tetrahedra between the Dauphiné twin orientations below T_o that give rise to the coalescence of the line shape are also in part responsible for the decrease in the relaxation time observed.

The decrease in the ^{17}O quadrupolar asymmetry parameter (η) with increasing temperature, and the abrupt 1.5 order of magnitude drop in the ^{17}O T_1 across the transition is evidence for a similar mechanism occurring in cristobalite. The former can be best explained by a hopping of the oxygens among the twelve twin positions, resulting in an average position that is more symmetrical than the individual twin positions. The abrupt drop in T_1 at T_o is most likely due to a change in structural fluctuations – probably the point at which the fluctuations in the tetrahedra go from being long-range correlated to a unit cell scale. Thus, the transitions in both quartz and cristobalite are best described by the transition from long-range correlated fluctuations of the tetrahedra between twin related domains below the transition to shorter until cell scale fluctuations between twin related domains above the transition.

Acknowledgements. We graciously thank the reviewers, Subrata Ghose and Brian Phillips, for insightful comments and correcting errors in early drafts of the manuscript. We would also like to thank Brian Phillips for pointing out some inaccuracies in early data sets, for enlightening discussion, and for sharing unpublished data. In addition, we would like to thank Marty Wolf of the Center for Materials Research thermal analysis lab at Stanford for assistance in the DSC measurements. This research was supported under National Science Foundation grants EAR 85-53024 and EAR 89-05188.

References

Abragam A (1961) Principles of nuclear magnetism. Oxford University Press, Oxford

Anderson PW (1954) A mathematical model for the narrowing of spectral lines by exchange or motion. J Phys Soc Japan 9:316–339

Avogadro A, Rigamonti A (1973) Nuclear spin-lattice recovery laws and an experimental condition for an exponential decay. In: Hovi V (ed) XVII Congress Ampere. Elsevier, North-Holland, pp 255–259

Avogadro A, Bonera G, Borsa F, Rigamonti A (1974) Static and dynamic properties of the structural phase transitions in $NaNbO_3$. Phys Rev B 9:3905–3920

Axe JD, Shirane G (1970) Study of the α-β phase transformation by inelastic neutron scattering. Phys Rev B 1:342–348

Bachheimer JP (1980) An anomaly in the β phase near the α-β transition of quartz. J Phys Lett 41:L-559–L-561

Blinc R, Burgar M, Rutar V, Seliger J, Zipancic I (1977) ^{31}P chemical-shift study of the ferroelectric transition in KD_2PO_4. Phys Rev Lett 38:92–95

Blinc R, Zupancic I, Lahajnar G, Slak J, Rutar V, Verbec M, Zumer S (1980) ^{31}P chemical shift and relaxation study of the pseudo-one-dimensional ferroelectric transition in CsD_2PO_4. J Chem Phys 72:3626–3629

Blinc R (1981) Magnetic resonance and relaxation in structurally incommensurate systems. Phys Rep 75:331–398

Borsa F, Rigamonti A (1990) Comparison of NMR and NQR studies of phase transitions in disordered and ordered crystals. In: Muller KA, Thomas H (eds) Structural Phase Transitions II. Springer, Berlin Heidelberg New York, pp 83–175

Boysen H, Dorner B, Grimm H (1980) Dynamic structure determination for two interacting modes at the M-point in α- and β-quartz by inelastic neutron scattering. J Phys C 13:6127–6146

Cox RT (1977) Optical absorption of the d^4 ion Fe^{4+} in pleochroic amethyst quartz. J Phys C 10:4631–4643

Devreux F, Boilot JP, Chaput F, Sapoval B (1990) NMR determination of the fractal dimension in silica aerogels. Phys Rev Lett 65:614–617

Dollase WA (1965) Reinvestigation of the structure of low cristobalite. Z Kristallogr 121:369–377

Engelhardt G, Radeglia R (1984) A semi-empirical quantum-chemical rationalization of the correlation between SiOSi angles and ^{29}Si NMR chemical shifts of silica polymorphs and framework aluminosilicates (zeolites). Chem Phys Lett 108:271–274

Engelhardt G, Michel D (1987) High-resolution solid-state NMR of silicates and zeolites. Wiley, Chichester

Farnan I, Stebbins JF (1990) High-temperature ^{29}Si NMR investigation of solid and molten silicates. J Am Chem Soc 112:32–39

Fyfe CA (1983) Solid state NMR for chemists. C.F.C Press, Guelph

Ghiorso MS, Carmichael ISE, Moret LK (1979) Inverted high-temperature quartz: Unit cell parameters and properties of the α-β inversion. Contrib Mineral Petrol 68:307–323

Gibbs GV (1982) Molecules as models for bonding in silicates. Am Mineral 67:421–450

Harris RK (1983) Nuclear magnetic resonance spectroscopy. Pitman, London

Hartman JS, Rigby SS, Sliwinski DR (1992) Non-exponential silicon-29 spin-lattice relaxation in synthetic silicate minerals. Trans Am Geophys Union 73:334

Hatta I, Matsuura M, Yao H, Gouhara K, Kato N (1985) True behavior of heat capacity in α, incommensurate and β phases of quartz. Thermochim Acta 88:143–148

Hatch DM, Ghose S (1991) The α-β phase transition in cristobalite, SiO_2. Phys Chem Minerals 17:554–562

Heaney PJ, Veblen DR (1991) Observations of the α-β phase transition in quartz: a review of imaging and diffraction studies and some new results. Am Mineral 76:1018–1032

Hill VG, Roy R (1958) Silica structure studies: V, the variable inversion in cristobalite. J Am Ceram Soc 41:532–537

Höchli UT, Scott JF (1971) Displacement parameter, soft-mode frequency, and fluctuations in quartz below its α-β phase transition. Phys Rev Lett 26:1627–1629

Janseen R, Tijink AH, Veeman WS, Maesen ThLM, van Lent JF (1989) High-temperature NMR study of zeolite Na-A: detection of a phase transition. J Phys Chem 93:899–904

Kihara K (1990) An X-ray study of the temperature dependence of the quartz structure. Eur J Mineral 2:63–77

Kirkpatrick RJ (1988) MAS-NMR spectroscopy of minerals and glasses. In: Hawthorne FC (ed) Spectroscopic Methods in Mineralogy and Petrology. Mineralogical Soc Am Rev Mineral, 18, pp 405–427

Leadbetter AJ, Smith TW (1976) The α–β transition in the cristobalite phases of SiO_2 and $AlPO_4$ II. Calorimetric studies. Philos Mag 33:113–119

Le Chatelier H (1889) Sur la dilatation du quartz. Comptes Rendus de l'Académie des Sciences 108:1046–1049

Liebau F, Böhm H (1982) On the co-existence of structurally different regions in the low-hi-quartz and other displacive phase transformations. Acta Crystallogr A38:252–256

Lippmaa E, Mägi M, Samoson A, Engelhardt G, Grimmer A-R (1980) Structural studies of silicates by solid-state high-resolution ^{29}Si NMR. J Am Ceram Soc 102:4889–4893

Liu SB, Pines A, Brandriss M, Stebbins JF (1987) Relaxation mechanisms and effects of motion in albite ($NaAlSi_3O_8$) liquid and glass: a high temperature NMR study. Phys Chem Minerals 15:155–162

Müller VD (1982) Zur Bestimmung chemischer Verschiebungen der NMR-Frequenzen bei Quadrupolkernen aus den MAS-NMR-Spektren. Ann Phys 39:451–460

Narita K, Umeda J, Kusumoto H (1966) Nuclear magnetic resonance powder patterns of the second-order nuclear quadrupolar interaction in solids with asymmetric field gradient. J Chem Phys 44:2719–2723

Navrotsky A, Geisinger KJ, McMillan P, Gibbs GV (1985) The tetrahedral framework in glasses and melts – inferences from molecular orbital calculations and implications for structure, thermodynamics, and physical properties. Phys Chem Minerals 11:284–298

Nieuwenkamp W (1937) Über die Struktur von Hoch-Cristobalit. Z Kristallogr 96:454–458

Peacor DR (1973) High-temperature single-crystal study of the cristobalite inversion. Z Kristallogr 138:274–298

Perrotta AJ, Grubbs DK, Martin ES, Dano NR (1989) Chemical stabilization of β-cristobalite. J Am Ceram Soc 72:441–447

Phillips B, Kirkpatrick RJ, Thompson JG (1990) ^{27}Al and ^{31}P NMR spectroscopy of the α-β transition in $AlPO_4$ cristobalite: evidence for a dynamical order-disorder transition. Trans Am Geophys Union 71:1671

Pluth JJ, Smith JV, Faber Jr J (1984) Crystal structure of low cristobalite at 10, 293, and 473 K: variation of framework geometry with temperature. J Appl Phys 57:1045–1049

Radeglia R, Engelhardt G (1985) Correlation of Si-O-T (T=Si or Al) angles and ^{29}Si chemical shifts in silicates and aluminosilicates. Interpretation by semi-empirical quantum-chemical considerations. Chem Phys Lett 114:28–30

Raman CV, Nedungadi TMK (1940) The α-β transformation of quartz. Nature 145, 147

Rigamonti A (1984) NMR-NQR studies of structural phase transitions. Adv Phys 33:115–191

Shapiro SM, O'Shea DC, Cummins HZ (1967) Raman scattering study of the alpha-beta phase transition in quartz. Phys Rev Lett 19:361–364

Smith JV, Blackwell CS (1983) Nuclear magnetic resonance of silica polymorphs. Nature 303:223–225

Spearing DR, Stebbins JF (1989) The ^{29}Si shielding tensor in low quartz. Am Mineral 74:956–959

Spearing DR, Farnan I, Stebbins JF (1990) NMR lineshape and T_1 relaxation study of the α-β phase transitions in quartz and cristobalite. Am Geophys Union Trans 71:1671

Stebbins JF, Farnan I, Williams EH, Roux J (1989) Magic angle spinning NMR observations of sodium site exchange in nepheline at 500° C. Phys Chem Minerals 16:763–766

Stebbins JF (1991) Nuclear magnetic resonance at high temperature. Chem Rev (in press)

Tezuka Y, Shin S, Ishigame M (1991) Observation of the silent soft phonon in β-quartz by means of hyper-raman scattering. Phys Rev Lett 66:2356–2359

Timken HKC, Turner GL, Gilson J-P, Welsh LB, Oldfield E (1986a) Solid-state oxygen-17 nuclear magnetic resonance spectroscopic studies of zeolites and related systems. 1. J Am Chem Soc 108:7231–7235

Timken HKC, Janes N, Turner GL, Lambert SL, Welsh LB, Oldfield E (1986b) Solidstate oxygen-17 nuclear magnetic resonance spectroscopic studies of zeolites and related systems. 2. J Am Chem Soc 108:7236–7241

Tse D, Lowe IJ (1968) Nuclear spin-lattice relaxation in CaF_2 crystals via paramagnetic centers. Phys Rev 166:292–302

Tsuneyuki S, Aoki H, Tsukada M, Matsui Y (1990) Molecular-dynamics study of the α to β structural phase transition of quartz. Phys Rev Lett 64:776–779

Tuttle OF (1949) The variable inversion temperature of quartz as a possible geologic thermometer. Am Mineral 34:723–730

van Goethem L, van Landuyt J, Amelinckx S (1977) The α-β transition in amethyst quartz as studied by electron microscopy and diffraction. Phys Status Solidi A 41:129–137

Van Kranendonk J, Walker M (1967) Theory of quadrupolar nuclear spin-lattice relaxation due to anharmonic raman phonon processes. Phys Rev Lett 18:701–703

van Tendeloo G, van Landuyt J, Amelinckx S (1976) The $\alpha \rightarrow \beta$ transition in quartz and $AlPO_4$ as studied by electron microscopy and diffraction. Phys Status Solidi A 33:723–735

Weber MJ (1963) Temperature dependence of spin-lattice relaxation in alkali halides. Phys Rev 130:1–10

Welberry TR, Hua GL, Withers RL (1989) An optical transform and monte carlo study of the disorder in β-cristobalite, SiO_2. J Appl Crystallogr 22:87–95

Wemmer DE (1978) Some double resonance and multiple quantum NMR studies in solids. PhD thesis, University of California, Berkeley

Withers RL, Thompson JG, Welberry TR (1989) The structure and microstructure of α-cristobalite and its relationship to β-cristobalite. Phys Chem Minerals 16:517–523

Wright AF, Leadbetter AJ (1975) The structures of the β-cristobalite phases SiO_2 and $AlPO_4$. Philos Mag 31:1391–1401

Wright AF, Lehmann MS (1981) The structure of quartz at 25 and 590° C determined by neutron diffraction. J Solid State Chem 36:371–380

Wyckoff RWG (1925) The crystal structure of the high temperature form of cristobalite (SiO_2). Am J Sci 9:448–459

Xiao Y, Kirkpatrick RJ, Phillips BL (1992) ^{29}Si MAS NMR investigation of $\alpha \leftrightarrow \beta$ phase transition in cristobalite. Trans Am Geophys Union 73:361

Young RA (1962) Mechanism of the phase transition in quartz. Report 2569, Air Force Office of Scientific Research, Washington, DC

Young RA, Post B (1962) Electron density and thermal effects in alpha quartz. Acta Crystallogr 15:337–346